Desert locust dynamics: Behavioral phase change and swarming

Chad Topaz *, Maria D'Orsogna †, Leah Edelstein-Keshet ‡, and Andrew Bernoff §

*Macalester College, St. Paul, U.S.A.,† California State University, Northridge, U.S.A.,‡ University of British Columbia, Vancouver, Canada, and § Harvey Mudd College, Claremont, U.S.A.

Submitted to Proceedings of the National Academy of Sciences of the United States of America

The African Locust Schistocerca gregaria is known to have two interconvertible phases, solitary and gregarious. Individuals are repelled (attracted) by others depending on their solitary (gregarious) state, and crowding tends to bias conversion towards the gregarious form. Here we model the spatio-temporal interactions and transitions between the two phases using nonlocal (integropartial) differential equations. We use steady state and linear stability analysis to characterize the conditions for onset of a locust "plague", characterized by mass transition to the gregarious form. Model reduction to approximate "bulk" theory allows us to quantify the size and density of the emergent gregarious clusters, and numerical simulations provide qualitative descriptions of the swarm structure.

locust | phase change | swarm | gregarious | solitary

Abbreviations:

utbreaks of the desert locust *Schistocerca gregaria* regularly afflict vast areas of northern Africa, the Middle East and southwest Asia. Depending on climate and vegetation conditions, billions of voracious locusts aggregate into destructive swarms that span areas up to a thousand square kilometers. A locust swarm can travel a few hundred kilometers per day, stripping crops and vegetation in its destructive path. [1–4]. The latest locust plague in West Africa (2003–2005) severely disrupted agriculture, destroying \$2.5 billion in crops destined for both subsistence and export. Despite control efforts totalling \$400 million, loss rates escalated to 50% in certain regions [5, 6]. These numbers alone attest to the urgency of finding better ways to predict, manage, and control locust plague outbreaks.

Between plagues, locusts are mainly solitary creatures who live in arid regions and lay eggs in small breeding grounds lush with vegetation. Occasionally, resources are abundant enough to support numerous hatchings, leading to a high density of adults. Overcrowding at resource sites promotes a transition to the gregarious phase, in a self-reinforcing process. The available supply of vegetation and water at the breeding ground is eventually exhausted, and locusts migrate *en masse* to other locations in search for nourishment. These newly formed locust swarms are able to keep their cohesiveness via direct sensory communication, chemical, and/or vibrational signaling [7–9]. Newly settled feeding grounds are also inevitably depleted, leading to several stop-and-go cycles of traveling locust bands. Outbreaks may be exacerbated in periods of drought, when large numbers of locusts congregate on the same breeding or feeding grounds.

Desert locusts are *phase polyphenic:* while sharing the same genotype, individuals may display different phenotypes [10, 11] such as morphology [12], coloration [13], reproductive features [14] and most significantly behavior [15, 16]. The latter can change from *solitary* where locusts seek isolation to *gregarious* where they attract one another. Behavioral state is plastic [3, 11, 15] and strongly dependent on local population density: in sparse surroundings, a gregarious locust transforms into the solitary state [15] and vice–versa in crowded environments. It is this phenotype switch that takes place when large numbers of locusts gather at a site, promoting a massive change from solitary to gregarious form and initiating the swarm plague [17, 18].

Locust gregarization is induced by visual and olfactory cues, but a most potent stimulus is tactile: repetitive stroking of the femora of hind legs [15, 16, 19] is believed to function as a crowding indicator. The mechanosensory stimulation of leg nerves leads to subsequent serotonin cascades in the brain, and in turn to the onset of gregarious behavior [16, 19, 20]. Furthermore, contact with individuals coming from behind enhances the tendency of a stationary locust to move [21]. In the laboratory, it has been shown that the solitary to gregarious switch can be induced by rubbing a locust's hind leg for 5 seconds per minute during a period of 4 hours [19]. Cessation of physical contact leads to a transition back to the solitary state after 4 hours.

There have been relatively few mathematical studies of locust behavior, especially of the switch between solitary and gregarious phases in a spatio-temporal framework. Both [22] and [23] studied the dynamics of rolling patterns formed by migrating locust groups. Data driven models include the self-propelled particle model of [24] where the observed transition between disordered to ordered locust movement was described via well-known physics paradigms [25]. A logistic map was introduced in [26] to describe population switching via a birth rate and a carrying capacity dependent on population density modulated by stochastic effects. None of the previous studies have focused on how an initially disperse, solitary locust population spontaneously transitions into an aggregated, gregarious one. The goal of this paper is to provide a mathematical description of such behavioral phase changes by taking into account the most relevant biological findings and by including relevant spatial features that cause locusts to clump or disperse.

OUR MAIN FINDING IS...

The model

As described above, locusts in a group are subject to attractive and/or repulsive forces based on combined sensory, chemical, and mechanical cues. Here we assume that such sensing is directionally isotropic, a simplification used in many similar models [29, 30]. We represent social forces as superimposed pairwise interactions and treat the locust population density $\rho(\mathbf{x},t)$ (rather than individual locusts) using a continuum approach. This standard representation provides us with analytical tools that can be brought to bear on the problem of characterizing the initiation and structure of a swarm. Our framework is based on a common model for a swarm, given by

$$\rho_t + \nabla \cdot (\rho \mathbf{v}) = 0, \quad \mathbf{v} = -\int_{\Omega} \nabla \mathbf{Q}(\mathbf{x} - \mathbf{x}') \rho(\mathbf{x}', t) \, d\mathbf{x}'$$
 [1]

Reserved for Publication Footnotes

where $\mathbf{x} = (x, y)$ (e.g., in 2D) and the velocity \mathbf{v} of an individual at (\mathbf{x},t) depends on attraction-repulsion social interactions with density of others in its vicinity. Such interactions are depicted as a convolution with a social interaction field $Q(\mathbf{x} - \mathbf{x}')$ that describes the influence of the population at location \mathbf{x}' on that at location \mathbf{x} . We use the notation $\mathbf{v} = -\nabla Q * \rho$ for the above convolution and assume that Q is radially symmetric. Eqn. [1] has been extensively studied, including work in [31–34]. Generally, solutions to Eqn. [1] include distinct regimes such as static (steady state) swarms, spreading, and blow-up [27]. Compactly supported 1D steady state swarms with and without jump discontinuities at their edges have been analyzed in depth in [28].

To adapt Eqn. [1] to biphasic desert locust swarm dynamics, we denote the density of solitary and gregarious locusts by $s(\mathbf{x},t)$ and $g(\mathbf{x},t)$ respectively, and the total density by $\rho=s+g$. We also include the density-dependent rate $f_1(\rho)$ to describe locust phenoptype switches from the gregarious to the solitary state and $f_2(\rho)$ for the opposite transition. We thus arrive at

$$\dot{s} + \nabla \cdot (v_s s) = -f_2(\rho)s + f_1(\rho)g,$$
 [2a]

$$\dot{g} + \nabla \cdot (v_g g) = f_2(\rho) s - f_1(\rho) g,$$
 [2b]

where the velocities are given by

$$v_s = -\nabla(Q_s * \rho), \quad v_g - \nabla(Q_g * \rho).$$
 [3]

In order to model the crowd-avoidance of solitary locusts we take pure social repulsion. Gregarious locusts, on the other hand are assumed to be attracted to others at long legnth scales and repelled at shorter ones, in order to avoid the artifact of infinitely dense clustering. Hence, we take the solitary gregarious interaction fields Q_s and Q_g to be

$$Q_s(\mathbf{x}) = R_s e^{-|\mathbf{x}|/r_s}, \quad Q_q(\mathbf{x}) = R_q e^{-|\mathbf{x}|/r_g} - A_q e^{-|\mathbf{x}|/a_g}.$$
 [4]

The parameters in Q_g must be chosen in the clumping regime, per the conditions stated in [27]. Specifically, we require $R_g a_g - A_g r_g > 0$ so that repulsion dominates at short length scales, and $A_g a_g^2 R_g r_g^2 > 0$ so that attraction dominates at longer ones. We model $f_{1,2}$ via Hill-type functions so that

$$f_1(\rho) = \frac{\delta_1}{1 + (\rho/k_1)^2}, \quad f_2(\rho) = \frac{\delta_2 (\rho/k_2)^2}{1 + (\rho/k_2)^2}.$$
 [5]

These choices allow the gregarious to solitary transition rate f_1 to be a decreasing function of ρ and f_2 to increase with ρ , saturating at $delta_2$. Here δ_i are maximal rates (units of 1/hr) and k_i are characteristic locust densities at which the phase change occurs at 1/2 of its maximal rate. The model we study consists of Eqs. [2]-[5]. We study these in 2D and 1D, with appropriate boundary conditions in a finite domains with initial conditions that specify $s(\mathbf{x}, 0)$ and $g(\mathbf{x}, 0)$, and hence both $\rho(\mathbf{x}, 0)$ and the total mean density $\rho_0 = \int \rho(\mathbf{x}, 0) d\mathbf{x}$.

Biological Parameter Values

We draw upon the experimental results of [19] to estimate phase change parameters in [5]. Phase change from the gregarious to solitarious state takes approximately four hours, and vice versa. Thus, $\delta_1 = \delta_2 = 1/4 = 0.25 \; h^{-1}$. The critical density for gregarization is 50 - 80 locusts /m². We assume that the solitarization process has the same critical density, setting $k_1 = k_2 \approx 65$ locusts /m².

To estimate social interaction range parameters in [4], we apply results of [24, 35], identifying the "sensing range" of a locust as 0.14 m, and the "repulsion range" as 0.04 m, on order with the approximately 0.08 m body length of a mature individual. We set our repulsion length scales $r_s = r_g = 0.04$ m, corresponding to the experimental repulsion range. Since attraction typically operates over longer scales, we take $a_g=0.14$ m, corresponding to the experimental sensing range.

We find R_s , R_g , and A_g from explicit computations of velocity under our model. The speed of a locust when it is alone varies from 72 - 216 m/hr, depending on diet [35]. At the upper end, this is roughly 1 body length per second. When it is moving in a group, the speed varies in a tighter range of 144 - 216 m/hr [35]. To estimate R_s we imagine the hypothetical semi-infinite density field $\rho(x) = \rho_0 H(x)$. Here, H(x) is the Heaviside function and $\rho_0 = 65$ locusts /m², the approximate critical density of a gregarious group. A solitarious locust placed at the origin, at the swarm's edge, should move to the left with maximal velocity $v_s^{max} = -216$ m/hr. We use the velocity definition Eq. [3] to write

$$v_s(0,0) = -\partial_x \left\{ Q_s * \rho_0 H(x) \right\} \Big|_{(0,0)} = v_s^{max},$$
 [6]

which we solve to find $R_s = 11.87$ locusts \cdot m²/hr. Similarly, a gregarious locust at the origin should move to the right with maximal velocity $v_q^{max} = 216$ m/hr, and so

$$v_g(0,0) = -\partial_x \left\{ Q_g * \rho_0 \mathbf{H}(x) \right\} \Big|_{(0,0)} = v_g^{max}.$$
 [7]

A gregarious locust placed a short distance away from the swarm equal to the attraction length scale should also move to the right, but with a slower velocity which we take to be the minimal velocity in a crowd, $v_g^{min} = 144$ m/hr. Thus

$$v_g(-0.14) = -\partial_x \left\{ Q_g * \rho_0 \mathbf{H}(x) \right\} \Big|_{(-0.14,0)} = v_g^{min}.$$
 [8]

Together, these two conditions determine $R_g = 5.13 \text{ locusts} \cdot \text{m}^2/\text{hr}$ and $A_q = 13.33$ locusts m²/hr.

Homogeneous steady states

For any set of initial conditions, the mean locust density ρ_0 is known, and corresponds to the the total density at the homogeneous steady state. Accordingly, there is a family of homogeneous steady states parameterized by the total homogeneous density ρ_0 . The densities of solitarious and gregarious forms are then

$$s_0 = \frac{\rho_0 \delta_1 k_1^2 (k_2^2 + \rho_0^2)}{\delta_1 k_1^2 k_2^2 + \delta_1 k_1^2 \rho_0^2 + \delta_2 k_1^2 \rho_0^2 + \delta_2 \rho_0^4}$$
 [9a]

$$g_0 = \frac{\delta_2 \rho_0^3 (k_1^2 + \rho_0^2)}{\delta_1 k_1^2 k_2^2 + \delta_1 k_1^2 \rho_0^2 + \delta_2 k_1^2 \rho_0^2 + \delta_2 \rho_0^4}.$$
 [9b]

In the small ρ_0 limit,

$$s_0 \approx \rho_0 - \beta \rho_0^3$$
, $g_0 \approx \beta \rho_0$, $\beta = \frac{\delta_2}{\delta_1 k_2^2}$ [10]

and thus the low-density steady state is composed mostly of solitarious locusts. In the large ρ limit,

$$s_0 pprox rac{1}{eta
ho_0}, \quad g_0 pprox
ho_0 - rac{1}{eta
ho_0},$$
 [11]

and thus the high-density steady state is composed mostly of gregarious locusts. These estimates already point to the nonmonotonicity of s_0 with total density.

Further evidence of this relationship is given in Fig. 1 where s_0, g_0 are shown as functions of the total density ρ_0 . To obtain the three sets of curves, we took a uniform distribution around each parameter, centered at the value estimated based on biological data, with a range from 0.7 to 1.3 times this mean value. We drew 10,000 sample parameter sets and plotted three pairs of curves, corresponding to 25, 50, and 75 percentile levels of the steady state value of s_0 (in blue) and g_0 (in green).

As noted, s_0 at first increases with ρ_0 , as both solitarious and gregarious locusts accumulate. Beyond some total density, s_0 reaches a maximum and starts to decrease, whereas g_0 keeps growing. From a biological point of view, this model prediction implies that homogeneous solitary groups can only exist up to some total density, beyond which gregarization dominates. While for the chosen functions f_i , closed form expression for the maximum cannot be obtained, the special case $k_1=k_2=k$ and $\delta_1=\delta_2=\delta$ (as in our biologically estimated parameters) leads to $\max(\rho_0,s_0)=(k,k/2)$.

[PUT IN SUPPLEMENT?] We can look for an approximate solution when $k_{1,2}$ and $\delta_{1,2}$ are each slightly detuned from equality. The basic idea is to expand everything in a power series in a small parameter ϵ . Take the formula for s_0 from Eq. 9a, differentiate it, and set it equal to zero to look for the critical point. This is our governing equation. Then expand everything in a power series. Without loss of generality, we can do this as

$$k_1 = k + \epsilon K, \quad k_2 = k - \epsilon K,$$
 [12a]

$$\delta_1 = \delta + \epsilon \Delta, \quad \delta_2 = \delta - \epsilon \Delta,$$
 [12b]

$$\rho_0 = \rho_{00} + \epsilon \rho_{01}. \tag{12c}$$

Substituting the power series into the equation for s' and solving at $\mathcal{O}(1)$ and $\mathcal{O}(\epsilon)$ yields

$$\rho_{00} = k, \quad \rho_{01} = K + \frac{\Delta k}{\delta}.$$
[13]

Thus, the maximum solitarious density occurs at $\rho_0 \approx k + K + \Delta k/\delta$. Substituting back into the original formula for s_0 and keeping through $\mathcal{O}(\epsilon)$ gives us the maximum steady state solitarious density, which is $s_{max} \approx k/2 + \Delta k/(2\delta)$.

I've checked how good this approximation is vis-a-vis the parameter sensitivities. That is, I've set k=65 and $\delta=0.25$. I've let the deviation K be as large as 0.3k and the deviation Δ be as large as 0.3δ – that is, I've considered up to 30% deviation from the mean values. Comparing the exact (numerical) values for the critical point's coordinates to the approximate values, you get up to 20% error for the ρ_0 coordinate and 15% error for the s coordinate.

Another interesting feature of the graph of s_0 and g_0 is that there is a point of equality between the two curves. By setting $s_0 = g_0$ in Eq. 9 and rejecting the trivial case $\rho_0 = 0$, one finds one positive solution, which is that $s_0 = g_0$ when

$$\rho_0 = \frac{k_1}{2\delta_2} \left(\delta_1 - \delta_2 + \sqrt{(\delta_1 - \delta_2)^2 + 4\delta_1 \delta_2 (k_2/k_1)^2} \right).$$
 [14]

This solution is exact (no assumptions or approximations are necessary). In the white and grey region of Fig. 9, $s_0 > g_0$ at the 50th percentile, and the reverse is true in the pink region. The solid, vertical purple lines lines show the 25th and 75th percentile of the equality point.

Linear stability analysis

To study stability of the steady state solution, we consider small perturbations, s_1, g_1, ρ_1 . Set

$$s(\mathbf{x},t) = s_0 + s_1(\mathbf{x},t), \quad g(\mathbf{x},t) = g_0 + g_1(\mathbf{x},t),$$
 [15]

$$\rho(\mathbf{x},t) = \rho_0 + \rho_1(\mathbf{x},t) = s_0 + g_0 + s_1(\mathbf{x},t) + g_1(\mathbf{x},t).$$
 [16]

Substitute Eqn. [15] and Eqn. [16] into [2], assume s_1 and g_1 are small, *i.e.*, $\mathcal{O}(\epsilon)$, and Taylor expand through $\mathcal{O}(\epsilon)$ to obtain the linearized equations

$$\dot{s}_1 = s_0 Q_s * \nabla^2 (s_1 + g_1) - A s_1 + B g_1,$$
 [17a]

$$\dot{g}_1 = g_0 Q_q * \nabla^2 (s_1 + g_1) + A s_1 - B g_1$$
 [17b]

where

$$A = f_2(\rho_0) + f_2'(\rho_0)s_0 - f_1'(\rho_0)g_0$$
 [18a]

$$B = f_1(\rho_0) + f_1'(\rho_0)g_0 - f_2'(\rho_0)s_0.$$
 [18b]

Since f_1 is monotonically decreasing and f_2 is monotonically increasing, $f_1'(\rho_0) < 0$ and $f_2'(\rho_0) > 0$ (excluding the trivial possibility ρ_0 =0). Hence, A, B > 0.

To further analyze the equations, Fourier expand the perturbations as

$$s_1(\mathbf{x},t) = \sum_{\mathbf{k}} \mathcal{S}_{\mathbf{k}}(t) e^{i\mathbf{k}\cdot\mathbf{x}}, \quad s_2(\mathbf{x},t) = \sum_{\mathbf{k}} \mathcal{G}_{\mathbf{k}}(t) e^{i\mathbf{k}\cdot\mathbf{x}}.$$
 [19]

The admissible wave vectors \mathbf{k} depend on the chosen domain Ω . In the event that $\Omega = \mathbb{R}^n$ then all \mathbf{k} are admissible (per the Fourier transform). Substituting into Eqn. [17] yields a set of ordinary differential equations for each Fourier mode amplitude. These are conveniently written in matrix form. Dropping the subscripts on $\mathcal S$ and $\mathcal G$ for simplification of notation, we have

$$\frac{d}{dt} \begin{pmatrix} \mathcal{S} \\ \mathcal{G} \end{pmatrix} = \mathbf{L}(k) \begin{pmatrix} \mathcal{S} \\ \mathcal{G} \end{pmatrix}, \quad [20a]$$

$$\mathbf{L}(k) \equiv \begin{pmatrix} -s_0 k^2 \widehat{Q}_s(k) - A & -s_0 k^2 \widehat{Q}_s(k) + B \\ -g_0 k^2 \widehat{Q}_g(k) + A & -g_0 k^2 \widehat{Q}_g(k) - B \end{pmatrix}. \quad \textbf{[20b]}$$

Here, $k = |\mathbf{k}|$ is the perturbation wave number, and $\widehat{Q}_{s,g}(k)$ are the Fourier transforms of the social interaction potentials, that is,

$$\widehat{Q}_s(k) = 2\pi \frac{R_s r_s^2}{(1 + r_s^2 k^2)^{3/2}},$$
 [21a]

$$\widehat{Q}_g(k) = 2\pi \left[\frac{R_g r_g^2}{(1 + (r_g^2 k^2)^{3/2}} - \frac{A_g a_g^2}{(1 + a_g^2 k^2)^{3/2}} \right]$$
.[21b]

The eigenvalues of L(k) are

$$\lambda_1(k) = -k^2 \left[s_0 \widehat{Q}_s(k) + g_0 \widehat{Q}_g(k) \right], \quad \lambda_2 = -(A+B).$$
 [22]

The eigenvalue λ_2 is negative since A,B>0. Thus, the constant density steady state is stable if $\lambda_1(k)<0$ for all admissible k. If $\lambda_1(k)>0$ for some k, then the constant density steady state is unstable to perturbations of those wave numbers. Crucially, this pivotal eigenvalue $\lambda_1(k)$ does not depend on the functions $f_{1,2}$ which describe behavioral phase change. It only depends on the social interaction potentials and on the relative mean densities of solitary and gregarious locusts.

We can further analyze this eigenvalue. The possible unstable wave numbers k are those satisfying $\lambda_1(k)>0$, where

$$\lambda_1(k) = -2\pi k^2 \times$$

$$\left[\frac{s_0 R_s r_s^2}{(1 + k^2 r_s^2)^{3/2}} + \frac{g_0 R_g r_g^2}{(1 + k^2 r_g^2)^{3/2}} - \frac{g_0 A_g a_g^2}{(1 + k^2 a_g^2)^{3/2}} \right]$$

where we have substituted for $\widehat{Q}_g(k)$ and $\widehat{Q}_s(k)$. [CHECK THAT THIS IS FOR 2D POTENTIALS AND SAY THAT.]

In order to make analytical progress we set $k_1 = k_2 = h$ and $\delta_1 = \delta_2 = \delta$. The use of h is to avoid confusion with the wavelength k. We also use the fact that $r_s = a_g$. These equalities all hold for our biologically estimated parameters. Later it will be useful to recall that within our model $r_g < r_s$. Inserting these simplifications, we find

$$\lambda_1(k) = \frac{2\pi R_g \rho_0^3 r_g^2 k^2}{(h^2 + \rho_0^2)(1 + k^2 r_s^2)^{3/2}} [M - m(k)]$$
 [24]

where

$$M = \frac{\rho_0^2 A_g r_s^2 - h^2 R_s r_s^2}{R_g \rho_0^2 r_g^2}, \quad m(k) = \frac{(1 + k^2 r_s^2)^{3/2}}{(1 + k^2 r_g^2)^{3/2}}.$$
 [25]

Since m(k) > 0, for instability to occur we must require M > 0, otherwise $\lambda_1(k)$ will always be negative. This necessary (but not sufficient) condition translates to

$$\rho_0 > \sqrt{\frac{R_s}{A_g}} h$$
 [26]

which in our case for $R_s=11.87, A_g=13.3$ (units of locusts m²/hr) and h=65 /m²[UNITS OK?] implies that if $\rho_0\leq 61.4$ locusts/m², the system is stable to perturbations of all wave numbers. This provides the critical density for clustering and swarm initiation.

Let us now look at the terms inside the square brackets of Eqn. [24]. We know that $r_q < r_s$. This implies that the function m(k) is monotonically increasing. Hence, for $\lambda_1(k)$ to be positive, it is also necessary that M be greater than the minimum value of m(k), attained at k=0. Thus, a more stringent condition is that

$$M > m(k = 0) = 1.$$
 [27]

Using the fact that $m(k \to \infty) = r_s^3/r_q^3 > 1$ we can now distinguish three cases:

- if M < 1 then $\lambda(k) < 0$ and the homogeneous steady state is stable to perturbations of all wave numbers.
- if $1 \leq \hat{M} \leq r_s^3/r_g^3$ then instabilities will arise for perturbations with wave numbers in a band extending from k = 0 to some finite
- if $M>r_s^3/r_g^3$ then the system is unstable to perturbations of any wave number.

The condition M > 1 that guarantees instability can be rewritten as

$$\rho_0 > \left(\frac{R_s}{A_a - R_a (r_a/r_s)^2}\right)^{1/2} h$$
[28]

so that, we are now guaranteed instability as long as $\rho_0 > 61.4$, close to the 50th percentile value of $\rho_0 = 57.5$ in Fig. 1, which is the left border of the grey region. [CHAD IS CONSIDERING: WHY AREN'T THEY CLOSER?] The vertical black dashed lines indicate the 25th and 75th percentile values for the onset of instability. Note that at the 50th percentile level, instability occurs before g_0 overtakes

Fig. 2 shows the most unstable wave number k_{max} as a function of ρ_0 . This wavenumber would be characterize the cluster diameter of the swarm as it is first initiated. [BRIEFLY EXPLAIN HOW **OBT'D**]. For low densities, the most unstable wavenumber is 0, indicating that large wavelength aggregation zones destabilize first. As ρ_0 increases, there is a sharp transition region in which k_{max} grows rapidly. Here, clusters of some finite size would be seen. We further observe that k_{\max} levels to a plateau value. (As before, the three curves in Fig. 2 are the 25th, 50th, and 75th percentile values as parameters are varied). At the 50th percentile value the large ρ_0 asymptotic value of k_{max} is $k_{max} = 8.9$. [GIVE UNITS AND INDICATE PREDICTED CLUSTER DIAMETERS.]

Maximum Instability [INCLUDE IN SUPPLEMENT?]

Bulk theory for segregated states

In simulations of [2], we observe mass-balanced states in which gregarious and solitarious locusts spatially segregate. We can approximate this behaviour with the following "bulk" state model reduction. For convenience, define the total number of solitary locusts and gregarious locusts,

$$S = \int_{\Omega} s \, d\Omega, \quad G = \int_{\Omega} g \, d\Omega,$$
 [29]

the total population mass M = S + G, and the mass fractions

$$\phi_s = S/M, \quad \phi_g = G/M, \quad \phi_s + \phi_g = 1.$$
 [30]

We assume that solitarious locusts are spread throughout most of the domain Ω , covering an area denoted α_s , whereas gregarious locusts clumped in a region whose area we call α_g . (This area can be estimated from the gregarious potential; see [4].) Then in these regions, local densities are approximately

$$s = S/\alpha_s, \qquad g = G/\alpha_g.$$
 [31]

For a segregated steady state at mass balance, the number flux of gregarious locusts becoming solitarized per unit time, $Gf_1(G/\alpha_q)$, should equal the number flux of solitarious locusts becoming gregarized, $Sf_2(S/\alpha_s)$. Equating these and substituting from [5]

$$\frac{\delta_2 S^3}{\alpha_s^2 k_o^2 + S^2} = \frac{\delta_1 k_1^2 \alpha_g^2 G}{\alpha_g^2 k_1^2 + G^2}.$$
 [32]

Solving [32] using [30] and dividing by M yields

$$\frac{c_1 \phi_s^3}{1 + c_2 \phi_s^2} = \frac{c_3 \phi_g}{1 + c_4 \phi_g^2}.$$
 [33]

where

$$c_1 = \frac{\delta_2 M^2}{\alpha_s^2 k_2^2}, \qquad c_2 = \frac{M^2}{\alpha_s^2 k_2^2}, \qquad c_3 = \delta_1, \qquad c_4 = \frac{M^2}{\alpha_g^2 k_1^2}.$$

Discussion

TEMPORARY.. TO BE WRITTEN AFTER RESULTS COL-

LECTED] A recent general review of models for aggregation based on attraction and repulsion is provided by [36]. Purely theoretical models for swarming include integro-differential equations [9]. Application of such ideas to flying locust swarms include [22] and [23].

As far as marching locusts, there have been a number of studies in which data collected in the laboratory and theoretical models have been combined. Most models concerned with alignment of locusts moving in a group [24, 37, 38] as well as proportion of locusts moving at a given time [21, 35] depending on treatments such as diet and denervation. The motivation in many of these models is to explore the transition between a disordered and a coherent marching group capable of great destructive force. [37] formulated an abstract model of collective motion, with repulsion and attraction that was then modified by [35] for locusts. The authors describe an individual-based model with locust in 2 states (stopped, moving) with stochastic transitions. They consider that locusts sense others in a spatial range and that this leads to an escape-dominated response with a parameter χ that reflects the strength of social interactions. They take a repulsive range of 2 cm and assume that the strength of the repulsion is $\chi_r = 10 \text{cm/s}^2$. They write a Langevin equation for the speed and orientation of each locust. The main output of the model is proportion of individuals moving and mean group speed as a function of the group density. (The mean group speed varies sigmoidally (over the range 0-7 cm/sec) with density in the range of 0-100 locusts /m².

ACKNOWLEDGMENTS. This work was supported by National Science Foundation Grant DMS-1009633 (to C.T.) and an NSERC Discovery grant (to LEK). We are grateful to the Mathematical Biosciences Institute where portions of this research were performed.

References

- 1. Kennedy JS (1951) The migration of the desert locust (*Schistocerca gregaria Forsk*). *Proc Roy Soc Lond B* 235:163–290.
- Albrecht FO (1967) Les grands problemes de la biologie, in Polymorphisme phasaire et biologie des acridiens migrateurs (Masson, Paris).
- 3. Uvarov B (1977) *Grasshoppers and locusts* (Cambridge Univ Press, London) Vol. 2.
- Rainey RC (1989) Migration and Meteorology: Flight Behavior and the Atmospheric Environment of Locusts and other Migrant Pests, Oxford Science Publications (Clarendon Press, Oxford).
- Bell M (2005) The 2004 desert locust outbreak. Bull Am Meteor Soc 86:S60.
- Brader L, et al. (2006) Towards a more effective response to desert locusts and their impacts on food security, livelihoods and poverty: Multilateral evaluation of the 2003–05 desert locust campaign, (United Nations Food and Agriculture Organization), Technical report.
- 7. Breder CM (1954) Equations descriptive of fish schools and other animal aggregations. *Ecol* 35:361–370.
- 8. D'Orsogna MR, Chuang YL, Bertozzi AL and Chayes L (2006) Self-propelled particles with soft-core interactions: patterns, stability and collapse. *Phys Rev Lett* 96:104302.
- 9. Mogilner A, Edelstein-Keshet L (1999) A non-local model for a swarm. *J Math Biol* 38:534–570.
- Applebaum SW, Heifetz Y (1999) Density-dependent physiological phase in insects. Ann Rev Entomol 44:317–341.
- 11. Pener MP, Simpson SJ (2009) Locust phase polyphenism: An update. *Adv Insect Physiol* 36:1 272.
- 12. Dirsh VM (1953) Morphometric studies on phases of the desert locust (Schistocerca gregaria Forskal. Antilocust Bull 16:1–34.
- Islam MS, Roessingh P, Simpson S J and McCaffery AR (1994b)
 Parental effects on the behavior and coloration of nymphs of the desert locust Schistocerca gregaria. J Insect Physiol 40:173–181.
- Schmidt GH and Albutz R (1999) Identification of solitary and gregarious populations of the desert locust, Schistocerca gregaria, by experimental breeding. *Entomol Gen* 24:161–175.
- Simpson SJ, McCaffery AR, Hagele BF (1999) A behavioral analysis of phase change in the desert locust. *Biol Rev* 74:461– 480.
- Rogers S, et al. (2003) Mechanosensory-induced behavioural gregarization in the desert locust schistocerca gregaria. *J Exp Bio* 206:3991–4002.
- Despland E, Collett M, Simpson S (2000) Small-scale processes in desert locust swarm formation: how vegetation patterns influence gregarization. *Oikos* 88:652–662.
- Collett M, Despland E, Simpson S, Krakauer D (1998) Spatial scales of desert locust gregarization. *Proc Natl Acad Sci* 95:13052.
- Simpson SJ, Despland E, Hagele BF, Dodgson T (2001) Gregarious behavior in desert locusts is evoked by touching their back legs. *Proc Natl Acad Sci* 98:3895–3897.

- Anstey ML, Rogers SM, Ott SR, Burrows M, Simpson SJ (2009) Serotonin mediates behavioral gregarization underlying swarm formation in desert locusts. *Science* 323:627–630.
- Bazazi S, Buhl J, Hale JJ, Anstey ML, Sword GA, Simpson SJ, Couzin ID (2008) Collective motion and cannibalism in locust migratory bands. *Curr Biol* 18:735–739.
- 22. Edelstein-Keshet L, Watmough J, Grunbaum D (1998) Do travelling band solutions describe cohesive swarms? An investigation for migratory locusts. *J Math Bio* 36:515–549.
- 23. Topaz CM, Bernoff AJ, Logan S, Toolson W (2008) A model for rolling swarms of locusts. *Eur Phys J Spec Top* 157:93–109.
- 24. Buhl J, Sumpter DJT, Couzin ID, Hale JJ, Despland E, Miller ER, Simpson SJ (2006) From disorder to order in marching locusts. *Science* 312:1402.
- 25. Czirøk, A et al (1995) Novel type of phase transition in a system or self-driven particles. *Phys Rev Lett* 75:1226–1229.
- Holt J, Cheke R (1996) Models of desert locust phase changes. *Ecol Model* 91:131–137.
- Leverentz AJ, Topaz CM and Bernoff AJ (2009) Asymptotic dynamics of attractive-repulsive swarms. SIAM J Appl Dyn Sys 8:880–908.
- 28. Bernoff AJ, Topaz CM (2011) A primer of swarm equilibria. SIAM J Appl Dyn Sys 10:212–250.
- Eftimie R, de Vries G, Lewis M A, Lutscher F (2007) Modeling group formation and activity patterns in self-organizing collectives of individuals. *Bull Math Biol* 69:1537–1565.
- Partan SR, Marler P, (2005) Issues in the classification of multimodal communication signals. Am Nat 166:231–245.
- 31. Bertozzi AL, Laurent T, (2009) The behavior of solutions of multidimensional aggregation equations with mildly singular interaction kernels. *Chi Ann Math Ser B* 30:463–482.
- 32. Bodnar M, Velasquez JJL, (2005) Derivation of macroscopic equations for individual cell-based models: a formal approach. *Math Meth Appl Sci* 28:1757–1779.
- Bodnar M, Velasquez JJL, (2006) An integro-differential equation arising as a limit of individual cell-based models. *J Diff Eq* 222:341–380.
- Topaz CM, Bertozzi AL, (2004) Swarming patterns in a twodimensional kinematic model for biological groups. SIAM J Appl Math 65:152–174.
- 35. Bazazi S, Romanczuk P, Thomas S, Schimansky-Geier L, Hale JJ, Miller GA et al. (2011) Nutritional state and collective motion: from individuals to mass migration. *Proc Roy Soc B* 278:356-363
- Schellinck J, White T (2011) A review of attraction and repulsion models of aggregation: Methods, findings and a discussion of model validation. *Ecol Mod* 222:1897–1911
- Romanczuk P, Couzin I, Schimansky-Geier L (2009) Collective motion due to individual escape and pursuit response. *Phys Rev Lett* 102:10602.
- 38. Yates AC, Erban R, Escudero C, Couzin ID, Buhl J, Kevrekidis IG et al (2009) Inherent noise can facilitate coherence in collective swarm motion. *Proc Natl Acad Sci* 106:5464–5469.

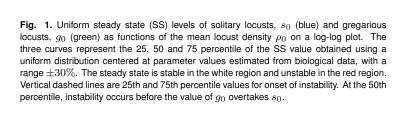


Fig. 2. Maximally unstable wavelength. At low densities, only the wavenumber $\boldsymbol{k}=\boldsymbol{0}$ is unstable. Near the critical density, k_{max} increases rapidly to some constant value as the density increases. Three curves correspond to same percentile values as in Fig 1